COBEM 2021 26th International Congress of Mechanical Engineering
November 22-26, 2021, Virtual Congress, Brazil

COB-2021-0017
VTR 4X4 THREE-DIMENSIONAL MATHEMATICAL MODEL WITH INDEPENDENT SUSPENSIONS AND MAGNETORHEOLOGICAL SHOCK ABSORBERS

Vilson Wenis dos Santos Belle
Ricardo Teixeira da Costa Neto
Instituto Militar de Engenharia, Praça General Tibúrcio 80, Rio de Janeiro, Brazil, 22290-270
e-mails vilson.belle@ime.eb.br, ricardo@ime.eb.br

Abstract. *A vehicle must be designed in such a way that it guarantees its occupants safety and comfort in the face of various situations, such as a sudden change of lane, something that can happen at any time during a trip or even a military operation. In this situation, the car must be able to react to this regretful excitement without compromising the car's stability. In this context, the present work aims to study the application of semi active suspension with magnetorheological dampers assisted by an embedded electronics system in order to improve the dynamic behavior of the vehicle, whose suspension springs are modeled in a non-linearly way using polynomials. To this end, this study performs an analysis of the vertical and lateral dynamics of a 4 x 4 vehicle with 10 degrees of freedom. The model construction uses the power flow methodology to establish the relationship between the kinematics and the dynamics of the chassis. And the computational implementation of the model was made by means of a block diagram, using a commercial software*

Keywords: *passive suspension, semi-active suspension, magnetorheological damper, vehicle dynamics*

1. INTRODUCTION

Maneuvers of sudden lane changes are recurrent in both the military and civilian world. They can be performed for a variety of reasons, the need to overtake quickly, avoid an accident and even circumvent problems on the track. Therefore, it is the role of the engineer to come up with improvements to the car in order to provide greater safety in carrying out this maneuver, avoiding the problems of loss of grip and rollover.
One of the solutions is to change the dampers, from traditional to magnetorheological. In order to carry out the feasibility analysis and to verify the possible improvement in the vehicle's damping, an analysis was made in the 4 x 4 vehicle when making a sudden double change maneuver, comparing through simulations the behavior of the body when using the two types of dampers. The three-dimensional vehicle with 10 degrees of freedom, 6 for the chassis and one for each suspension, was modeled in a Matlab/Simulink 2020 computational environment using the power flow methodology to establish the causal relationships between the different subsystems (Costa Neto, 2008). The simulations use the fourth order Runge Kutta, with a step of 0.01 seconds. The mathematical relations of force and movement are modeled based on the methodology developed in the works of Jazar (2014), Gillespie (1992), and Wong (2008).
The kinematic relationships that relate to the movement of the chassis, modeled as a rigid three-dimensional body, are based on the theory presented in Haug (1989) and that follows the spatial references of the ISO 4130 standard. To obtain one more accurate modeling, a non-linear tire behavior and analyzing the lateral forces with the magic formula (Pacejka et al., 1989). Although there are many other more modern models this one is used because is simple to implement, the tire parameters are relatively simple to find and, in addition, this equation can be easily linearized, this would facilitate the implementation of other control strategies in future research, such as a robust control with H^{∞} synthesis. The springs for vehicle suspensions are composed of a system that has, in a simplified way, one linear spring and two polymeric stops (Reimpell, 2001).
Among the various magnetorheological dampers models, such as Bingham, BouncWen, modified Bounc-Wen and hyperbolic tangent (Kwok, 2006), them the hyperbolic tangent is used. The control system used was the Fuzzy, which uses a fuzzy logic to control the current that feeds the shock absorber. The use of this type of control is due to the fact that the system is non-linear, due to the kinematic relationships of the chassis and the modeling of the tires. The simulations developed are related to the standardized test of double lane change, ISO 3888, by varying the speed of the vehicle in each test, it is possible to analyze the behavior of the various subsystems in the situation with the conventional shock absorber and the magnetorheological one.

2. TIRE MODEL

When you want to make a turn, the driver will steer the steering wheel according to the maneuver. This steering goes through a steering mechanism that causes the front wheels of the vehicle to steer. When a wheel is steered, a pointing angle appears, shown in Figure 1 by the x-axis, and the direction of the tire speed. This angle, represented by the angle α, is called the angle of deviation or lateral sliding. If a rolling tire travels on a curved path, the tread elements that are not in direct contact with the ground remain undeformed, that is, they do not produce lateral forces. However, the moment these elements reach the ground they deform laterally, starting to generate forces. As the elements move along the contact region, the tendency is that the lateral forces tend to increase to the point where the lateral forces overcome the friction with the ground. From that moment on, the elements start to lose adhesion. It is important to note that the fact that the tire has a sliding region does not mean that there is a loss of grip with the ground (Neves, 2002).

The lateral forces developed by the tire depend on the lateral slip angle, the vertical force applied, the camber angle and parameters related to the tire's physical constitution. Several mathematical formulations that describe the behavior of the lateral force, for the present work the magic formula developed in 1987 by Bakker, Pacejka and Nyborg is used, which carried out a series of empirical tests to arrive at the formulation exposed in Equation 1.

$$F_{lat} = D\ sen\left(C\ arctan\left(B(\alpha + S_h) - \arctan\left(B(\alpha + S_h)\right)\right)\right) + S_v \tag{1}$$

The coefficients are calculated using:

$$D = \mu F_z \tag{2}$$

$$\mu = a_1 F_z + a_2 \tag{3}$$

$$B.C.D = a_1 sen(2\arctan\,(F_z/a_4))(1 - a_5|\gamma|) \tag{4}$$

$$C = a_0 \tag{5}$$

$$B = BCD/CD \tag{6}$$

$$E = a_6 F_z + a_7 \tag{7}$$

$$S_h = a_8\gamma + a_9 F_z + a_{10} \tag{8}$$

$$S_v = a_{11} Fz\gamma + a_{12} F_z + a_{13} \tag{9}$$

Let μ be the side friction coefficient, γ the camber angle, F_z the vertical force and the coefficients a_i the tire constants. The need then arises to calculate the value of the lateral slip angle to find the value of the lateral force. To calculate this angle, the parameters δ and β are defined, which are respectively the steering angles and the wheel sideslip angle, angle between the tire speed vector and the tire's longitudinal axis, both shown in Figure 1.

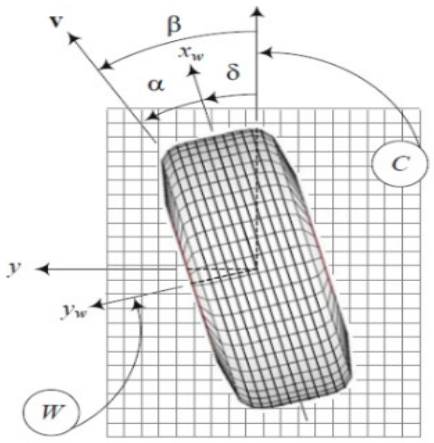

Figure 1.Tire reference and angles α, β e δ.

Therefore, the sideslip angle can be calculated by:

$$\alpha = \beta - \delta \tag{10}$$

Regarding the vertical dynamics of the tires, they are modeled as a trilinear spring: a region with zero force, which represents the situation of loss of contact with the ground, a region where the tire has a linear behavior in the compression of 0 to 0.1 meters and a region that represents the situation of excessive tire compression, a linear relation with an elastic constant much bigger.

3. SUSPENSION SPRINGS

The springs used in the suspension of a vehicle have a maximum working stroke, due to the system's spatial impediment. Polymeric bump and rebound stops are installed in the suspension to avoid either spring excessive elongation or compression in severe situations that could cause plastic deformation. Using the various graphics developed in Reimpell (2001) and adapting them to the vehicle used, in order to obtain satisfactory bump and rebound lengths, one arrives at the force curve developed by the spring as a function of the compression length of the system, as shown in Figure 2 and Equation 11, in which the force is given in kN and the length in meters.

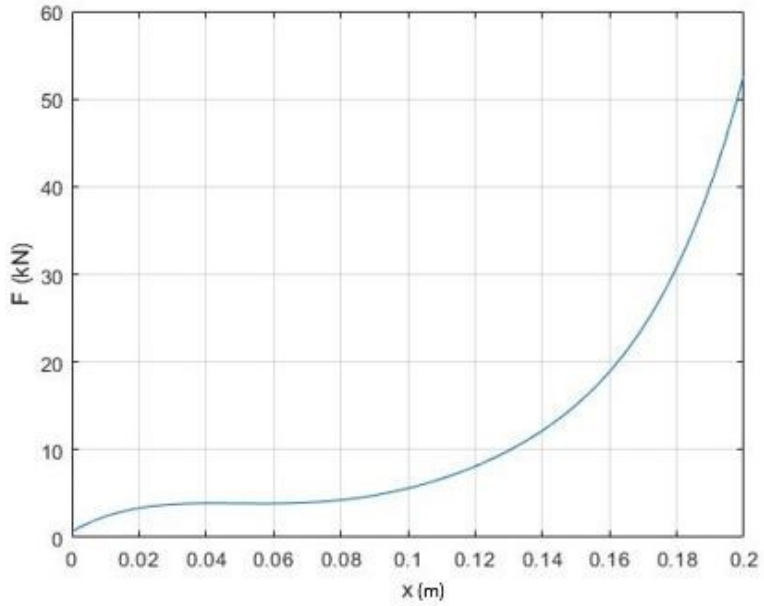

Figure 2. Force developed by the spring as a function of the deformation length.

$$F = 36 * 10^5 x^6 - 9 * 10^5 x^5 - 60207.3x^4 + 46138x^3 - 5171.9x^3 + 219.3x^2 + 0.6695 \quad (11)$$

4. MAGNETORHEOLOGICAL DAMPER

A Magnetorhelogical (MR) damper is usually made up of piston, magnetic coils, accumulators, bearings, seals and a reservoir with MR fluid. The operation of an MR damper is simply, basically the electric current, through the coil, controls the flow of fluid thus controlling the damping (Reimpell, 2001).

There are several models that try to predict nonlinear behavior of this type of damper. The one that faithfully meets the expected result and is mathematically simple and easy to implement in the model is the hyperbolic tangent model. While other models use differential equations, the model in this work uses of the hyperbolic tangent function to simulate the hysteresis and linear functions to represent viscosity and rigidity, this equation can be seen in Equation 12 (Kwok, 2006).

$$f = c\dot{x} + kx + \alpha \tanh\left(\beta\dot{x} + \delta sign(x)\right) + f_0 \quad (12)$$

Where x and $\dot{x}$ are the displacement and velocity of the piston MR damper, respectively; c and k are the viscous and stiffness coefficients, respectively; α is a scale factor of the hysteresis; β and δ are the parameters controlling the shape of the hysteresis loops; and f_0 is the damper force offset. The constants used in Kwok (2006) were obtained by testing real MR buffer and with varied frequencies, amplitudes and currents in the damper. Because of the impossibility of carrying out these tests, a linear regression will help to get them. Besides, the parameters are set as $k = 0, \beta = 100, \delta = 0$ and $f_0 = 0$, the exact same considerations are made in Dantas (2018) and Miranda (2020) and they are made to better

adapt this MR to the car without this resource, in order to better analysis the differences between these situations. Moreover, when the MR does not receive current the damping coefficient (c), corresponds to the normal damper. With these considerations and the relations in Kwok (2006), the others coefficients are:

$$c = 1929i + 3200 \tag{13}$$

$$\alpha = -244i^2 + 918i + 32 \tag{14}$$

$$\beta = 100 \tag{15}$$

According to Kwok (2006) the current passing through the damper cannot be greater than 2 A, so as not to damage it. It is necessary to work with a conservative safety factor, because the most severe situation will not be a double lane change, but passing through a hole or a sudden rise. Therefore, it is considered that the current value can't exceed about 1 A, so that in the most severe situations, which will not be simulated in this work, he can react more appropriately. The block diagram in Matlab/Simulink is shown in Figure 3.

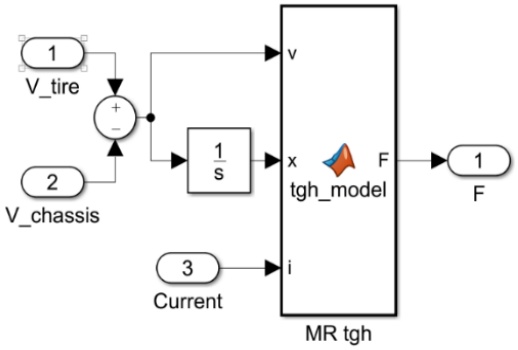

Figure 3. MR damper block diagram.

5. CONTROLLER SYNTHESIS

The Fuzzy Logic control is adopted to control each dumper, denoted by the subscript i. The objective is to reduce three points: the relative velocity between the unsprung mass and sprung mass X_{i1}, the velocity and acceleration of the chassis, respectively, X_{i2} and X_{i3}. The rule base consists in the logic IF-THEN rule statements. All inputs signals pass through the 'fuzzification' with three triangle functions within the range of -1 to 1, where N, Z and P represent, respectively, negative, zero and positive (Kurczyk, 2013).

Each inputs signal must be multiplied by constants to represent correctly the phenomenon, these constants are set by the behavior of the vehicle using passive dampers. In the Table 1 the results of the analysis are shown, where K_{rv} corresponds to the relative velocities gain, K_v denotes the absolute velocity gain and K_a describes the acceleration constant. Besides, it is necessary to use one other constant, denoted as K_i, to modify the scale of the output signal, the current, since the fuzzy's output is situated among zero and one.

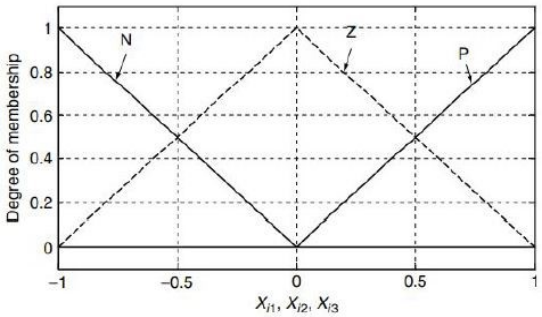

Figure 5. Input membership functions for fuzzy controller

Table 1: Gains used to adapt the problem to the fuzzy controller.

Parameter	Value
K_{rv}	1/0.5
K_v	1/0.5

K_a	1/7
K_i	1.8

The output signal is the current that feed the dumper and it is given in the form of singleton functions equally divided equally between zero and one. Therefore, I1 corresponds to the minimum (zero), I2=0.25, I3=0.5, I4=0.75 and I5=1 (the maximum value). In the Table 2 are showed the 27 rules utilized

Table 2: Logic relations in the fuzzy controller.

X_{i3}	N			Z			P		
$\frac{X_{i1}}{X_{i2}}$	N	Z	P	N	Z	P	N	Z	P
N	I5	I4	I2	I4	I1	I1	I3	I1	I1
Z	I1	I1	I1	I1	I1	I1	I1	I1	I1
P	I1	I1	I3	I1	I1	I4	I2	I4	I5

The block diagram is represented in the figure 6, showing the input signals, gains, MATLAB Fuzzy Logic Toolbox and the output signal.

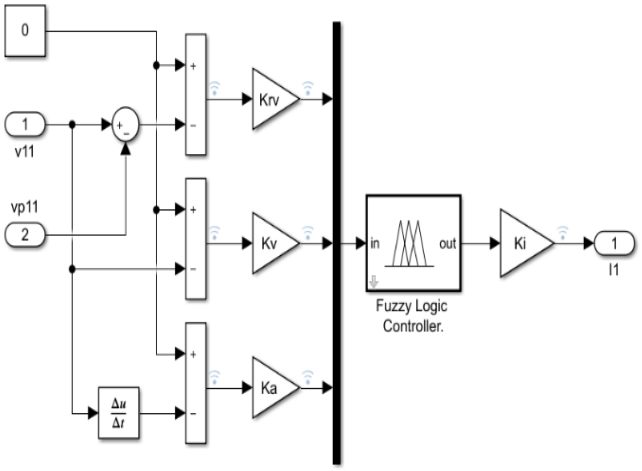

Figure 6. Control block diagram.

6. VEHICLE STEERING ANALYSIS

The steering mechanism used is the Ackerman system. This geometry creates a relationship between the steering angles of the external and internal wheels in order to allow that at low speeds the car makes a curve without sliding (Jazar, 2014, Gillespie, 1992 e Wong, 2008). This model can be represented mathematically by:

$$\cot(\delta_o) - \cot(\delta_i) = \frac{w}{l} \tag{17}$$

$$\cot(\delta) = \frac{(\cot(\delta_o) - \cot(\delta_i)}{2} \tag{18}$$

Where δ_o and δ_i are the steering angles of the inner and outer wheels of the curve, respectively, w is the width, l is the length and δ is defined as the average steering.

7. CHASSIS MODELING

In the model developed, the resulting efforts at the center of mass of the chassis are caused by the forces of each suspension at their respective anchorage points and the lateral forces developed by the tires. In Figure 7, the vehicle is represented as its degrees of freedom and the system constants, it serves as a reference for the mathematical development of the efforts and equations of movement of the chassis.

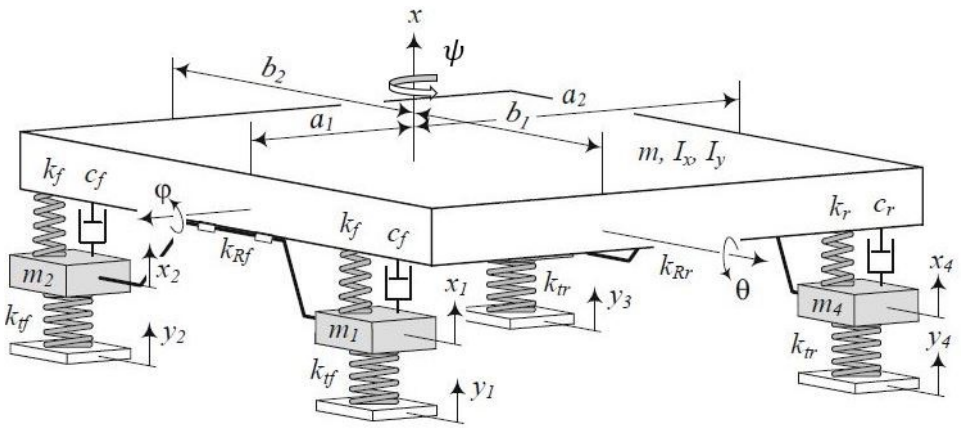

Figure 7. Full car model (Jazar, ,2014)

In relation to the forces coming from the suspensions, the power flow methodology can be used to calculate the efforts at the center of mass of the vehicle, so that:

$$\begin{bmatrix}\vec{F}\\ \vec{M}\end{bmatrix}_{susp} = \Theta^T \begin{bmatrix}\overrightarrow{F_{s1}}\\ \overrightarrow{F_{s2}}\\ \overrightarrow{F_{s3}}\\ \overrightarrow{F_{s4}}\end{bmatrix} \tag{19}$$

In this particular case, the suspension forces act only in the vertical direction, z axis of the adopted ISO standard. Therefore, we have:

$$\overrightarrow{F_{si}} = [0\ 0\ F_{si}]^T \tag{20}$$

Where F_{si} is the i (1, 2, 3 and 4) suspension force module. The matrix Θ is called the kinematic transformation matrix and is calculated by means of:

$$\Theta = \begin{bmatrix} I_{3x3} & -\widetilde{Tr}_1 \\ I_{3x3} & -\widetilde{Tr}_2 \\ I_{3x3} & -\widetilde{Tr}_3 \\ I_{3x3} & -\widetilde{Tr}_4 \end{bmatrix} \tag{21}$$

Where r_i is the position of the chassis anchor point, at the center of mass and T is the rotation matrix of the chassis center of mass, which is defined as:

$$T = T_x T_y T_z \tag{22}$$

In addition to the influence of suspensions, there is also the influence of tire forces on the chassis center of mass. The lateral force of the tire is developed in the tire frame, so it is necessary to apply a transformation of axles to take these forces to the frame, therefore:

$$\begin{bmatrix}F_{x1}\\ F_{y1}\end{bmatrix} = \begin{bmatrix}\cos(\delta_i) & -sen(\delta_i)\\ sen(\delta_i) & \cos(\delta_i)\end{bmatrix}\begin{bmatrix}0\\ F_{yw}\end{bmatrix} \tag{23}$$

When applying this same procedure to the 4 wheels, the tire forces are obtained in the vehicle's center of mass reference. To calculate the efforts, it is first possible to calculate the force and the resulting moment in the center of mass of the chassis. For the calculation of the result force, it is necessary to take these forces to the inertial frame, resulting in Equation 24.

$$\vec{F}_{pneu} = \begin{bmatrix} \cos(\psi) & -sen(\psi) & 0 \\ sen(\psi) & \cos(\psi) & 0 \\ 0 & 0 & 1 \end{bmatrix} \sum_{i=1}^{4} \begin{bmatrix} F_{xi} \\ F_{yi} \\ 0 \end{bmatrix} \tag{24}$$

While the resulting moment is calculated by means of the forces in the vehicle frame, which leads to Equation 26.

$$\vec{M}_{pneu} = \sum_{i=1}^{4} \widetilde{r_{i_t}} \begin{bmatrix} F_{xi} \\ F_{yi} \\ 0 \end{bmatrix} \tag{28}$$

Where r_{i_t} is the position of the i-th (1, 2, 3 and 4) tire in relation to the center of mass of the chassis. In addition to these factors, it is considered that there is an anti-roll bar in the vehicle. Therefore, the resulting stresses at the vehicle's center of mass are the sum of the stresses caused by the suspensions and the tires. From this result it is possible to calculate the accelerations, both linear and angular, of the chassis. By integrating linear and angular acceleration in relation to time, the linear and angular speeds of the chassis are obtained. From these values it is possible to use the kinematic transformation matrix to calculate the speeds of each anchorage point in the chassis.

$$\begin{bmatrix} \vec{v_1} \\ \vec{v_2} \\ \vec{v_3} \\ \vec{v_4} \end{bmatrix} = \Theta \begin{bmatrix} \vec{v}_{cm} \\ \vec{w}_{cm} \end{bmatrix} \tag{31}$$

The values of the chassis anchor points are used to calculate the reactions of the chassis in the suspension system, as well as the angles β necessary to calculate the lateral slip angle (equation 10). When integrating the linear velocity of the center of mass, its position is found as a function of time, however due to the model being three-dimensional, the integration of the angular velocity vector does not provide Euler angles. To calculate these angles, which are used in the analysis of the vehicle's behavior and in obtaining the kinematic transformation matrix, a series of transformations is applied based on the projections of these speeds based on the work of Haug (1989).

8. SIMULATIONS

There are a series of standards that standardize the double lane change tests, among them the ISO 3888 is chosen for the analysis of the model.

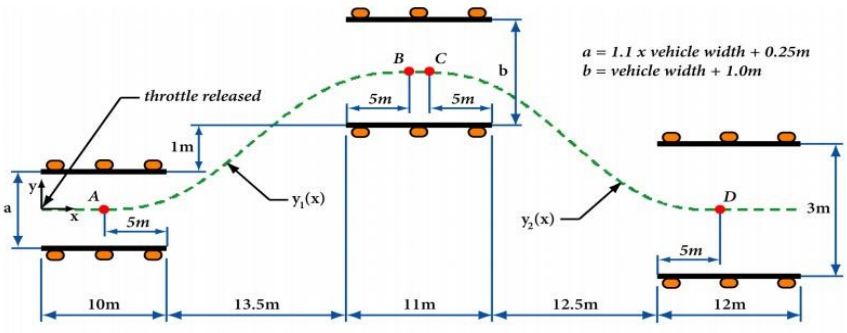

Figure 8. Road profile (Javali, 2013)

The driver model is essential to understand the vehicle's behavior. In this paper, the vehicle is able to maneuver in an open-loop system using the strategies adopted in Neves (2002) where the average steering angle (δ) is defined by:

$$\delta = 0, t < 6s \tag{32}$$

$$\delta = \frac{ang_{vol}\left[1 + \sin\left(\frac{2\pi(t-6)}{\Delta t}\right) - \frac{\pi}{2}\right]}{2}, 6 < t \leq t_{f1} \tag{33}$$

$$\delta = \frac{-ang_{vol}\left[1+\sin\left(\frac{2\pi(t-t_{f1})}{\Delta t}\right)-\frac{\pi}{2}\right]}{2}, t_{f1} < t \leq t_{f2} \quad (34)$$

$$\delta = 0, t_{f2} < t < t_{f3} \quad (35)$$

$$\delta = \frac{-ang_{vol}\left[1+\sin\left(\frac{2\pi(t-t_{f3})}{\Delta t}\right)-\frac{\pi}{2}\right]}{2}, t_{f1} < t \leq t_{f2} \quad (36)$$

$$\delta = \frac{ang_{vol}\left[1+\sin\left(\frac{2\pi(t-t_{f4})}{\Delta t}\right)-\frac{\pi}{2}\right]}{2}, t_{f1} < t \leq t_{f2} \quad (37)$$

$$\delta = 0, t \leq t_{f5} \quad (38)$$

The parameters of the vehicle and tires are represented in Table 3.

Table 3: Vehicle and tire parameters.

Vehicle Parameters	Value	Tire Parameters	Values
Chassis Mass	1715 kg	a_0	1.3
Front Wheel Mass	60 kg	a_1	2.117302
Rear Wheel Mass	75	a_2	1107.127089
Inertia axis y (I_y)	3865 $kg.m^2$	a_3	1815.614546
Inertia axis x (I_x)	638 $kg.m^2$	a_4	9.049286
Inertia axis z (I_z)	4035 $kg.m^2$	a_5	0
Dumper Conventional	3200 N s /m	a_6	0.379372
Câmber (γ)	0°	a_7	-4.060309
Center of gravity height (H)	0.60 m	a_8	0
a1	1.652 m	a_9	0
a2	-1.885 m	a_{10}	0
b1	0.7 m	a_{11}	0
b2	-0.7 m	$a_{12} = a_{13}$	0

First of all, the simulation is performed at a speed of 40 km/h. Figures 9 e 10 show the trajectory of the vehicles, center of mass and wheels, in the plane of road.

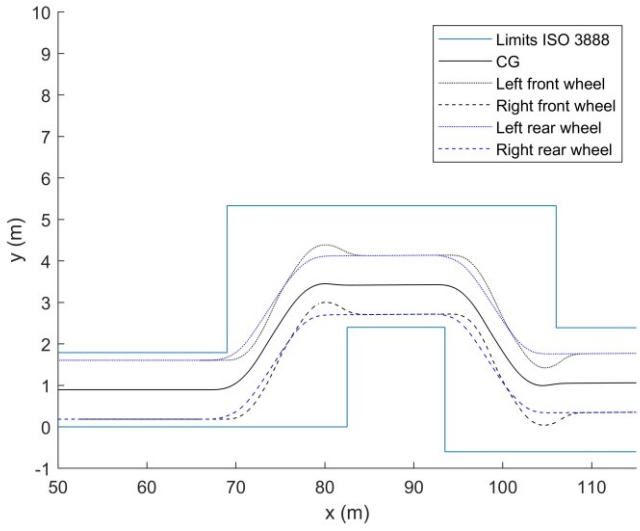

Figure 9. Vehicle trajectory at 40 km/h on the track with conventional dumpers

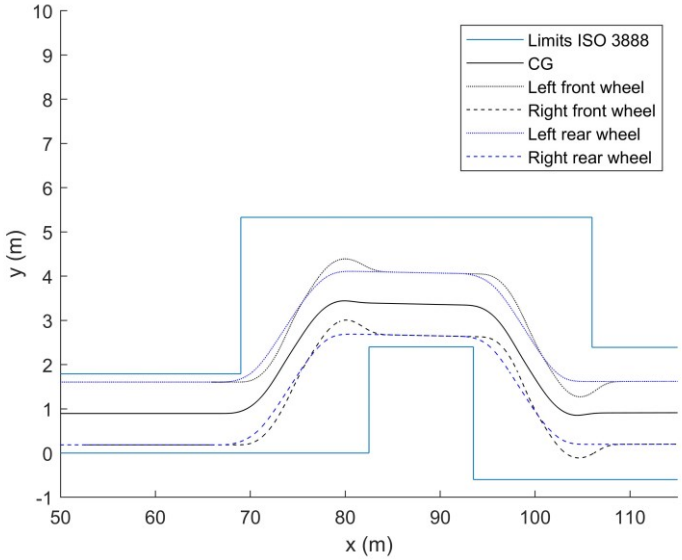

Figure 10. Vehicle trajectory at 40 km/h on the track with MR dumpers

It is evident both on trajectories with and without magnetorheological dampers that there were small slips at the end of the first and second lane changes, despite this on both occasions the vehicle was able to carry out the standard's trajectory. In Figure 11 there is a comparative analysis between the angles of roll in the situation with conventional shock absorber and with the control system. The roll angle is an important indicator in the analysis of the vehicle's stability during the turn, as very large roll angles indicate that the vehicle has a greater tendency to roll over. It can be seen that in the situation with a controller the scrolling amplitudes are smaller, which indicates a lesser tendency for the vehicle to roll over. Besides, the model with MR dampers provides a shorter oscillation period, since reaching the stable situation more quickly the car behaves better in the next steering, and also provides greater comfort to the occupants. To further analyze the possibility of overturning, the value of tire deformation during the maneuver is analyzed. When the deformation is equal to zero, the tire loses contact with the ground, which represents a threshold situation of loss of contact. Figure 12 shows the analysis of the right rear tire, which are the closest to the loss of contact.

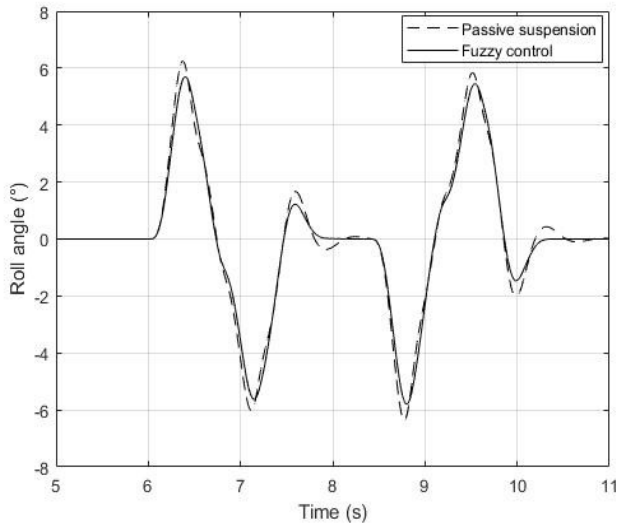

Figure 11. Rolling angles developed in the maneuver at 40 km/h with conventional and magnetorheological dampers

It is also possible to increase the speed of the vehicle in order to analyze this behavior in a more critical situation. To this end, a speed of 60 km / h is applied to the model. Figures 13 and 14 show the behavior of the vehicle in the plane of the track. It is noticed that at this speed the vehicle with conventional shock absorbers cannot perform the test stipulated by the standard, while the vehicle with the control system can.

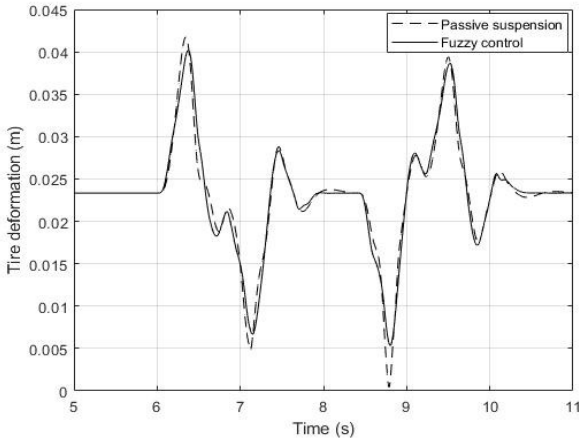

Figure 12. Deformation of the right rear tire during maneuvering at 40 km/h with conventional and magnetorheological shock absorbers

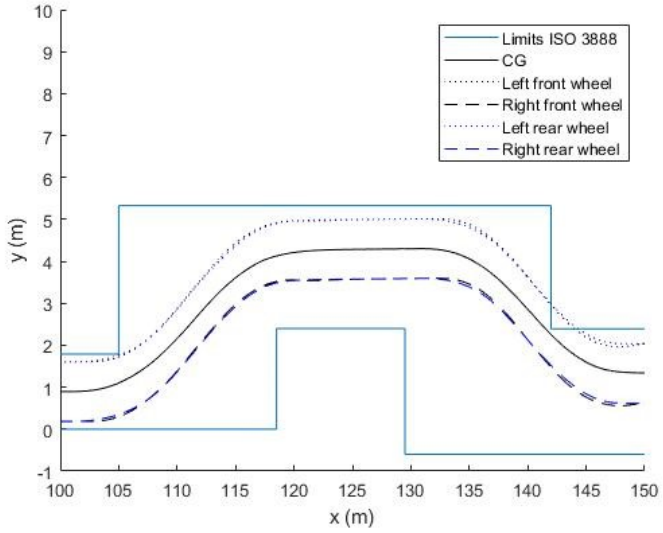

Figure 13. Vehicle trajectory at 60 km/h on the track with conventional dumpers

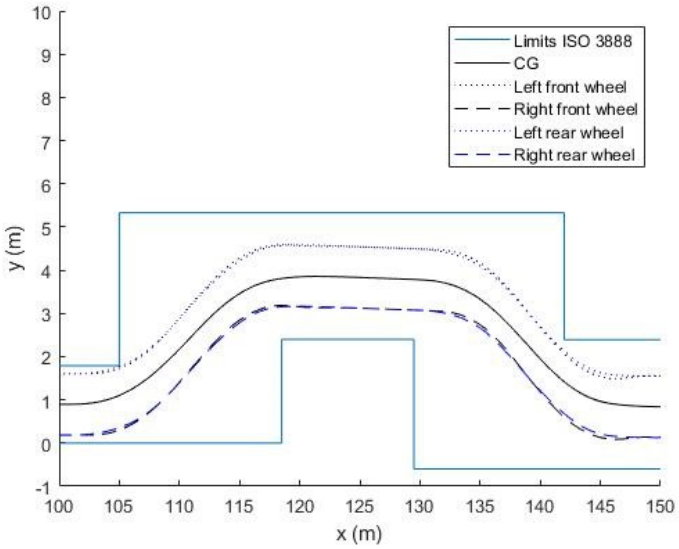

Figure 14. Vehicle trajectory at 60 km/h on the track with MR dumpers

When analyzing the right rear tire deformation curves during the maneuver, Figure 15, it is clear why the model with conventional shock absorbers cannot complete the course correctly, they lose contact with the ground over a period of time and this changes the dynamics of the system significantly, while with the controller the tires do not detach from the ground.

In figure 16, a comparison is made between the chassis roll angles, as expected, the suspension with MR dampers had a lesser variation, in addition to reaching balance more quickly. When comparing figure 16 with figure 11, it can be seen that the increase in speed caused a greater deviation from the scroll angle curves in models with and without MR, because at 40 km / h despite the small differences, the shape of the curve with the time was very similar. This difference is consistent with the other results of the model, since the model with passive suspension lost contact with the ground while the model with a controller did not, and this causes a difference in the dynamics of these models, even for a short period of time.

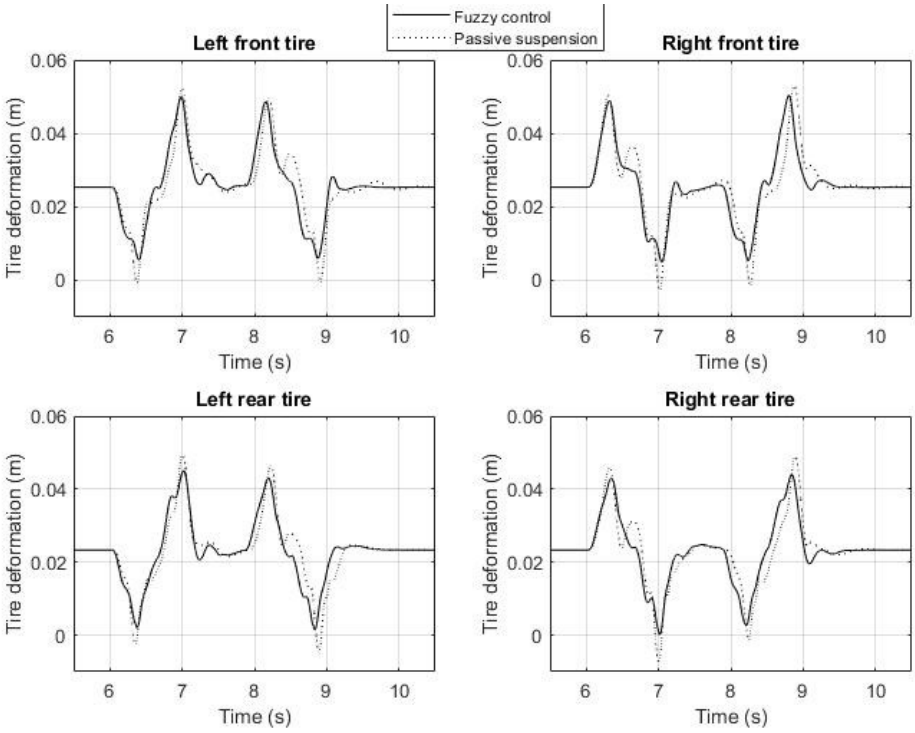

Figure 15. Deformation of the tires during maneuvering at 60 km/h with conventional and magnetorheological dumpers.

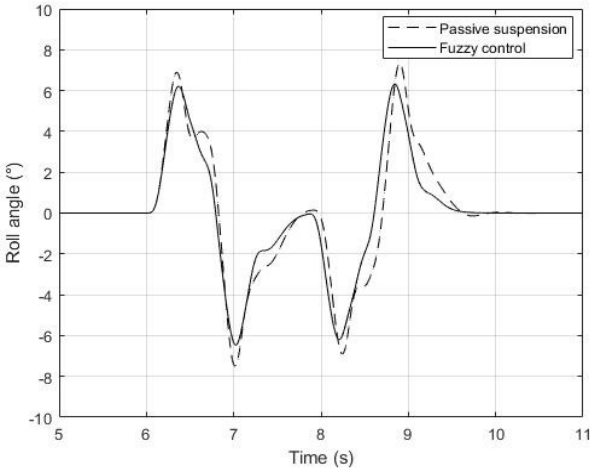

Figure 16. Rolling angles developed in the maneuver at 60 km/h with conventional and magnetorheological dampers

9. CONCLUSIONS

An analysis of the behavior of the vehicle model during the double lane change maneuver shows that the use of magnetorheological dampers improves the vehicle's performance in this situation, and it is even possible to carry out the test in a satisfactory way. It is still possible to verify that this improvement becomes more pronounced as the speed increases, since in the situation at 40 km/h as differences in behavior are not so marked as at 60 km/h. The methodology used in the block diagram proves to be very suitable for the situation, since from a change in the suspension blocks the comparative analysis of the models is facilitated, in addition to promoting a detailed analysis of each component of the vehicle. In addition, the Fuzzy control proves to be appropriate to the situation, because despite being a relatively simple control to implement, it is capable of working in a grid with several non-linearities. In conclusion, it can be said that the use of magnetorheological dampers provides greater stability for the vehicle during curves and, as a consequence, increases both the performance of the vehicle and the safety of the occupants.

10. REFERENCES

Matlab, M. The language of technical computing. The MathWorks, Inc, 2012. Available in: http://www mathworks.com.

Costa Neto, R.T., 2008. "*Modelagem e Integração dos Mecanismos de Suspensão e Direção de Veículos Terrestres Através do Fluxo de Potência"*, Doctoral Thesis, PUC-Rio

Jazar, R, N, 2014, *Vehicle Dynamics – Theory and Apllication*, 2nd ed., Springer.

Gillespie, T. D., 1992, *Fundamentals Of Vehicle Dynamics*, SAE.

Wong, J. Y., 2008, *Theory Of Ground Vehicles*, Wiley, 4ed.

HAUG, E. J., 1989, *Computer Aided Kinematcis and Dynamics Of Mechanical Systems. Vol 1*.

Bakker, E., Pacejka, H.B., Lidner, L. ,1989, *A New Tire Model with an Application in Vehicle Dynamics Studies*. 4th Auto Technologies Conference, Monte Carlo, 101-113, SAE paper 890087Rempeil

Reimpell, D. J., 2001, *The Automotive Chassis: Engineering Principles*, 2nd ed., B.H.

Kwok, N. et al., 2006. A novel hysteretic model for magnetorheological fluid dampers and parameter identification using particle swarm optimization. Sensors and Actuators A: Physical, Elsevier, v. 132, n. 2.

Neves, M. R. D. R., 2002." *ANÁLISE DA ESTABILIDADE LATERAL DE UM VEÍCULO TRIDIMENSIONAL*." 261 p. Master's degree in mechanical engineering — Instituto Militar de Engenharia, Rio de Janeiro.

Dantas, C., Gabriel, F., da Costa Neto, R., 2018. "*Influence of the distances between the axles in the vertical dynamics of a military vehicle equipped with magnetorheological dampers*", SAE Technical Paper 2018-36-0232.

Miranda, M., 2020. "*Performance of a vehicle on crawles on irregular land with suspensions equipped with magnetorreological shock absorbers*", SAE Technical Paper 2020-36-0145.

Kurczyk, S.; Paweczuk, 2013. M. Fuzzy control for semi-active vehicle suspension. Journal of Low Frequency Noise, Vibration and Active Control, v. 32, n. 3, p. 217–225.

Jalaki, K., Mcphee, J., Uchida, T. K., Lambert, S., 2013. "*Development of an Advanced Fuzzy Active Steering Controller and a Novel Method to Tune the Fuzzy Controller",* SAE Technical Paper 2013-01-0688.

11. RESPONSIBILITY NOTICE

The author(s) is (are) the only responsible for the printed material included in this paper.